A Family of [Ni$_8$] Cages Templated by μ$_6$-peroxide from Dioxygen Activation

Alexandros Perivolaris,[†] Constantinos C. Stoumpos,[†] Jolanta Karpinska,[‡] Alan G. Ryder,[‡] Jamie M. Frost,[§] Kevin Mason,[§] Alessandro Prescimone,[§] Alexandra M. Z. Slawin,[#] Vadim G. Kessler,[ʔ] Euan K. Brechin[§,*] and Giannis S. Papaefstathiou[†,*]

[†] Laboratory of Inorganic Chemistry, Department of Chemistry, National and Kapodistrian University of Athens, Panepistimiopolis, 157 71 Zografou, Greece.

[‡] Nanoscale Biophotonics Laboratory, School of Chemistry, National University of Ireland, Galway, Ireland.

[§] EaStCHEM School of Chemistry, The University of Edinburgh, West Mains Road, Edinburgh, EH9 3JJ, UK.

[#] School of Chemistry, The University of St. Andrews, Purdie Building, St. Andrews, Fife KY16 9ST, UK.

[ʔ] Department of Chemistry, Swedish University of Agricultural Sciences, Box 7015, 750 07 Uppsala, Sweden.

ABSTRACT: A family of exceptionally thermally stable [Ni$_8$] cages is reported, each being templated by a rare η^3:η^3:μ_6-O$_2^{2-}$ produced by dioxygen activation where the reducing agent for the O$_2$ reduction appears to be the ligand used in the reaction mixtures which was found within the nickel cages in its oxidized form.

INTRODUCTION

Dioxygen activation has provided substantial impetus for important developments in several different fields. This includes biomimetic and bioinorganic chemistry which aims to reveal the structures of the reactive intermediates at the active sites of metalloenzymes and give insights into the mechanistic details of dioxygen activation and oxygenation reactions,[1-6] and catalysis since the metal-dioxygen intermediates have been proposed as active oxidants in C–H bond activation reactions.[3]

It has been proposed that dioxygen activation first involves bonding of dioxygen at a reduced metal center to form metal-superoxo or metal-peroxo intermediates, followed by O···O bond cleavage leading to the formation of high-valent, metal-oxo species which are responsible for the oxidation reaction of the substrates within the metalloenzyme.[1-6] It is therefore believed that the presence of a redox-active metal center is a fundamental prerequisite for activating and reducing dioxygen.

Indeed, over the years, several high-valent metal-peroxo complexes, obtained by the act of dioxygen on a reduced metal center, have been structurally characterized by single-crystal X-ray crystallography.[4] These examples include Ti(IV)-peroxo,[4a] V(V)-peroxo,[4b] Cr(IV)-peroxo,[4c] Mn(III)-peroxo,[4d] Mn(IV)-peroxo,[4e] Fe(III)-peroxo,[4f] Co(III)-peroxo[4g-4k] and Cu(II)-peroxo[4l,4m] complexes that were isolated by the act of dioxygen on Ti$_2$(III), V(III), Cr(II), Mn(II), Mn(I), Fe(II), Co(II) and Cu(I) precursors, respectively.

Restricting further discussion to nickel-dioxygen species, there is only one Ni(II)-peroxo[5a] and one Ni(II)-superoxo[5b] compound obtained by the oxygenation of a Ni^0 and a Ni^I precursor, respectively, which have been structurally characterized. There are also few reports of spectroscopically characterized nickel-peroxo and nickel-superoxo complexes obtained by the act of dioxygen on low-valent Ni^0 and Ni^I precursors[2e,3a,6] while there are not any structurally characterized Ni(II)-peroxo species obtained by the act of dioxygen on Ni(II) centers.

Since Ni(II) is inert toward O$_2$, the most common approach to obtain Ni(II)-peroxo or Ni(II)-superoxo complexes is the use of H$_2$O$_2$.[5b] Indeed, there are a handful of structurally characterized Ni(II)-peroxo[7a,b] and Ni(II)-superoxo[7c,d] species obtained by the reaction of H$_2$O$_2$ with Ni(II) or Ni(III) precursors, respectively. It is worth noting that one Ni(II)-peroxo complex[8] has been obtained by the chemical reduction of a Ni(II)-superoxo precursor,[5b] with the latter being originally synthesized by the reaction of a Ni(I) precursor with O$_2$.

We herein report a family of [Ni$^{II}_8$] cages templated by a rare η^3:η^3:μ_6-O$_2^{2-}$ species produced by dioxygen reduction. Although we cannot ignore the presence of the Ni(II) ions, which might indeed be involved in the dioxygen activation, the reducing agent for the O$_2$ reduction appears to be the ligand used in the reaction mixtures, which was found within the nickel cages in its oxidized form. Specifically, three octanuclear Ni(II) cages, namely [Ni$_8$(O$_2$)(abmo)$_6$(MeCO$_2$)$_2$(MeO)$_6$(MeOH)$_4$]·4H$_2$O **1**·4H$_2$O, [Ni$_8$(O$_2$)(abmo)$_6$(PhCO$_2$)$_2$(MeO)$_6$(MeOH)$_4$]·2MeOH **2**·2MeOH and [Ni$_8$(O$_2$)(abmo)$_6$(4ClPhCO$_2$)$_2$(MeO)$_6$(MeOH)$_2$

$(H_2O)_2]$ **3**, (abmoH = α-benzilmonoxime, Chart 1) were isolated from the reaction of nickel(II) carboxylates with α-benzoin oxime (aboH$_2$, Chart 1) in MeOH under aerobic conditions. Interestingly, abmoH is the oxidized form of aboH$_2$. Direct evidence that the peroxide originates from the dioxygen reduction was provided by the act of $^{18}O_2$ in a deoxygenated reaction mixture of **2**. To the best of our knowledge, complexes **1-3** represent the first examples of structurally characterized Ni(II)-peroxo complexes obtained by the act of dioxygen on Ni(II) precursors.

Chart 1. The structures of α-benzoin oxime (aboH$_2$) and α-benzilmonoxime (abmoH).
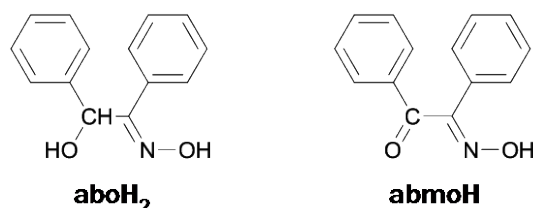
Such a dioxygen reduction where both the peroxide, O_2^{2-}, (*i.e.* the reduced species) and the oxidized species (*i.e.* the abmo$^-$) are isolated and structurally characterized in the final product, and in which the metal ion appears not to change its oxidation state, has never been observed. This means that the electrons needed to reduce the dioxygen into the O_2^{2-} are provided by the organic ligand (*i.e.* not the metal ion). The significance of these findings is that it provides evidence that the dioxygen activation and its subsequent reduction may also depend on the organic surroundings of the metal-containing active site of metalloenzymes.[1,2S,2t,2x] Nevertheless, there are few reports of structurally characterized metal-peroxo complexes obtained by dioxygen reduction where the metal center does not change oxidation state, but the reducing agent was not identified.[9] The same [Ni$_8$] cages can be isolated from the reaction of nickel(II) carboxylates with abmoH, but only when H$_2$O$_2$ is added into the reaction mixtures. One side product, namely [Ni$_5$(abo)$_2$(aboH)$_6$] ·4MeOH·CH$_2$Cl$_2$ **4·4MeOH·CH$_2$Cl$_2$** was also isolated and characterized by X-ray crystallography. To the best of our knowledge cages **1-3** represent the first polynuclear metal complexes which can be synthesized from different organic ligands (*i.e.* aboH$_2$ and abmoH).

EXPERIMENTAL SECTION

Materials and Methods. Ni(MeCO$_2$)$_2$·4H2O, aboH$_2$ (α-benzoin oxime) H$_2$O$_2$, Et$_3$N, KBr, $^{18}O_2$ (90%, ^{18}O-enriched) and H$_2$^{18}O$_2$ (2-3% solution, 90% ^{18}O-enriched) and all solvents were purchased from commercial sources and used as received. Ni(PhCO$_2$)$_2$·3H2O,[10] Ni(4ClPhCO$_2$)$_2$[10] (4ClPhCO$_2$H = 4-chloro-benzoic acid) and abmoH[11] (α-benzilmonoxime) were prepared according to literature procedures. IR spectra were recorded as KBr pellets in the 4000-400 cm^{-1} range on a Shimadzu FT/IR IRAffinity-1 spectrometer. TGA data were collected with a Mettler Toledo TGA/DCS1 instrument in 40 µl Al pans under a N$_2$ flow of 50 ml min^{-1}. Small sample portions (~1-2 mg) were used to avoid damage of the instrument due to the explo-

sive nature of the peroxide complexes. Variable-temperature, solid-state direct current (dc) magnetic susceptibility data down to 5 K were collected on a Quantum Design MPMS-XL SQUID magnetometer equipped with a 7 T dc magnet. Diamagnetic corrections were applied to the observed paramagnetic susceptibilities using Pascal's constants.

X-ray Crystallography. Data collection parameters and structure solution and refinement details are listed in Table 1. Full details for **1-4** can be found in the CIF files provided in the Supporting Information. Full crystallographic data for complexes **1-4** were collected from single-crystals obtained from aboH$_2$ (see Syntheses below). The structures of single-crystals obtained from abmoH were confirmed by measuring the cell dimensions.

Raman Spectroscopy. Raman spectra were collected for all samples on two different Raman spectrometers, both with 785 nm excitation. First a Raman Work-Station^{TM} (Kaiser Optical Systems Inc., Ann Arbor, MI) over a 200-3000 cm^{-1} spectral range, with a resolution of ~3-4 cm^{-1}. This system was equipped with a -40°C cooled CCD detector. The second system was a RamanStation spectrometer (AVALON Instruments Ltd, Belfast) equipped with a TE cooled (-90 °C) back thinned CCD detector. A laser power of ~70 mW (at the sample) with an exposure time of 2 × 10 seconds was generally used and spectra were collected from 250 to 3311 cm^{-1} (at a resolution of 4 cm^{-1}). For all data, exposure times (between 10 and 45 seconds) and accumulation numbers were varied in order to try and attain the optimal signal to noise (S/N) ratio in the Raman spectra so that any shifts in the peroxo bonds could be accurately measured. The spectra were not corrected for instrument response.

Mass spectrometry. The analysis was carried out using a Bruker Maxis Impact instrument with an electrospray (ESI-MS) ionisation source. The calibration solution used was Agilent ESI-L low concentration tuning mix solution, Part No. G1969-85000, enabling calibration between approximately 50 m/z and 2000 m/z. Samples were dissolved in CH$_2$Cl$_2$/CH$_3$OH at concentrations of 10^{-4} molL^{-1} and introduced into the MS at a dry gas temperature of 180 °C. The ion polarity for all MS scans recorded was positive, with the voltage of the capillary tip set at 4000 V, end plate offset at -500 V, funnel 1 RF at 400 Vpp and funnel 2 RF at 400 Vpp, hexapole RF at 200 Vpp, ion energy 5 eV, collision energy at 5 eV, collision cell RF at 1500 Vpp, transfer time at 120.0 µs and the pre-pulse storage time at 10.0 µs. Each spectrum was collected for 2 mins.

Syntheses

[Ni$_8$(O$_2$)(abmo)$_6$(MeCO$_2$)$_2$(MeO)$_6$(MeOH)$_4$]·4H$_2$O (1·4H$_2$O) and **[Ni$_5$(abo)$_2$(aboH)$_6$]·4MeOH·CH$_2$Cl$_2$ (4·4MeOH·CH$_2$Cl$_2$) from aboH$_2$.** To a slurry of Ni(MeCO$_2$)$_2$·4H$_2$O (0.4 mmol) and aboH$_2$ (0.4 mmol) in MeOH (25mL) was added a 1M Et$_3$N solution in EtOH (0.8 mmol). The slurry was stirred for 4 hours, during which time an orange-yellow precipitate formed in ~20% yield (based on Ni). The precipitate was filtered and the dark

green-brown filtrate left undisturbed for 4 days. Dark green single crystals of **1**·4H$_2$O were formed in ~55% yield (based on Ni). The crystals were collected by vacuum filtration, washed with a small amount of MeOH and Et$_2$O and dried in air. Recrystallization of the orange-yellow powder from CH$_2$Cl$_2$ / MeOH afforded orange-yellow crystals of **4**·4MeOH·CH$_2$Cl$_2$. Elemental analysis for **1**·4H$_2$O (%) calcd for C$_{98}$H$_{108}$N$_6$O$_{32}$Ni$_8$: C 50.05, H 4.63, N 3.57; found: C 50.10, H 4.50, N 3.53. Elemental analysis for **4**·4MeOH·CH$_2$Cl$_2$ (%) calcd for C$_{117}$H$_{112}$N$_8$O$_{20}$Cl$_2$Ni$_5$: C 60.71, H 4.88, N 4.84; found: C 60.69, H 4.82, N 4.80. IR for **1**·4H$_2$O, cm^{-1} (KBr pellets): 3052 w, 2923 w, 2810 w, 1583 s, 1551 s, 1444 sh, 1407 s, 1344 s, 1286 s, 1268 s, 1194 s, 1176 s, 1098 w, 1052 m, 1025 s, 999 w, 917 s, 793 br, 745 m, 719 w, 696 sh, 680 m, 642 w, 618 w, 582 w, 439 br. IR for **4**·4MeOH·CH$_2$Cl$_2$, cm^{-1} (KBr pellets): 1705 br, 1492 sh, 1452 sh, 1444 sh, 1138 br, 1111 br, 1069 sh, 1042 w br 1018 w br, 917 w, 835 w.

[Ni$_8$(O$_2$)(abmo)$_6$(PhCO$_2$)$_2$(MeO)$_6$(MeOH)$_4$]·2MeOH (2·2MeOH) and [Ni$_8$(O$_2$)(abmo)$_6$(4ClPhCO$_2$)$_2$(MeO)$_6$(MeOH)$_2$(H$_2$O)$_2$] (3) along with (4) were prepared in a similar manner with the above synthesis by replacing Ni(MeCO$_2$)$_2$·4H$_2$O with Ni(PhCO$_2$)$_2$·3H$_2$O and Ni(4ClPhCO$_2$)$_2$, respectively. The relevant yields for **2**·2MeOH and **4** were 60% and 15%, respectively, while those for **3** and **4** were 65% and 12%, respectively. Elemental analysis for **2**·2MeOH (%) calcd for C$_{110}$H$_{112}$N$_6$Ni$_8$O$_{30}$: C 53.54, H 4.57, N 3.41; found: C 53.50, H 4.53, N 3.44. IR for **2**·2MeOH, cm^{-1} (KBr pellets): 3049 w, 2917 w, 2812 w, 1588 s, 1547 s, 1444 sh, 1393 s, 1345 s, 1286 s, 1268 s, 1194 s, 1176 s, 1099 w, 1051 m, 1024 s, 998 w, 916 s, 800 w, 746 m, 719 m, 696 sh, 679 m, 640 w, 620 w, 582 w, 434 br. Elemental analysis for **3** (%) calcd for C$_{106}$H$_{98}$Cl$_2$N$_6$Ni$_8$O$_{28}$: C 52.08, H 4.04, N 3.44; found: C 50.05, H 4.00, N 3.49. IR for **3**, cm^{-1} (KBr pellets): 3055 w, 2920 w, 2813 w, 1587 s, 1546 s, 1444 m, 1396 s, 1345 s, 1286 s, 1269 s, 1193 s, 1176 s, 1096 w, 1051 m, 1027 m, 998 w, 916 s, 798 w, 775 w, 746 m, 718 w, 696 sh, 688 w, 582 w, 439 br.

[Ni$_8$(O$_2$)(abmo)$_6$(MeCO$_2$)$_2$(MeO)$_6$(MeOH)$_4$]·4H$_2$O (1·4H$_2$O) from abmoH. To a slurry of Ni(MeCO$_2$)$_2$·4H$_2$O (0.4 mmol) and abmoH (0.4 mmol) in MeOH (25mL) were added H$_2$O$_2$ (30% solution, 0.4 mmol) and Et$_3$N (1M solution in EtOH, 0.8 mmol). The slurry was stirred for 1 hour. The resulting dark green-brown solution was left undisturbed for 4 days. Dark green single crystals of **1**·4H$_2$O were formed in ~75% yield (based on Ni). The crystals were collected by vacuum filtration, washed with a small amount of MeOH and Et$_2$O and dried in air. Elemental analysis for **1**·4H$_2$O (%) calcd for C$_{98}$H$_{108}$N$_6$O$_{32}$Ni$_8$: C 50.05, H 4.63, N 3.57; found: C 50.12, H 4.53, N 3.52. IR for **1**·4H$_2$O, cm^{-1} (KBr pellets): 3052 w, 2923 w, 2810 w, 1583 s, 1551 s, 1444 sh, 1407 s, 1344 s, 1286 s, 1268 s, 1194 s, 1176 s, 1098 w, 1052 m, 1025 s, 999 w, 917 s, 793 br, 745 m, 719 w, 696 sh, 680 m, 642 w, 618 w, 582 w, 439 br.

[Ni$_8$(O$_2$)(abmo)$_6$(PhCO$_2$)$_2$(MeO)$_6$(MeOH)$_4$]·2MeOH (2·2MeOH) and [Ni$_8$(O$_2$)(abmo)$_6$(4ClPhCO$_2$)$_2$(MeO)$_6$(MeOH)$_2$(H$_2$O)$_2$] (3) were prepared in a similar manner with the above synthesis by replacing Ni(MeCO$_2$)$_2$·4H$_2$O with Ni(PhCO$_2$)$_2$·3H$_2$O and Ni(4ClPhCO$_2$)$_2$, respectively.

The relevant yields for **2**·2MeOH and **3** were 77% and 79%, respectively. Elemental analysis for **2**·2MeOH (%) calcd for C$_{110}$H$_{112}$N$_6$Ni$_8$O$_{30}$: C 53.54, H 4.57, N 3.41; found: C 53.52, H 4.54, N 3.43. IR for **2**·2MeOH, cm^{-1} (KBr pellets): 3049 w, 2917 w, 2812 w, 1588 s, 1547 s, 1444 sh, 1393 s, 1345 s, 1286 s, 1268 s, 1194 s, 1176 s, 1099 w, 1051 m, 1024 s, 998 w, 916 s, 800 w, 746 m, 719 m, 696 sh, 679 m, 640 w, 620 w, 582 w, 434 br. Elemental analysis for **3** (%) calcd for C$_{106}$H$_{98}$Cl$_2$N$_6$Ni$_8$O$_{28}$: C 52.08, H 4.04, N 3.44; found: C 50.07, H 4.02, N 3.45. IR for **3**, cm^{-1} (KBr pellets): 3055 w, 2920 w, 2813 w, 1587 s, 1546 s, 1444 m, 1396 s, 1345 s, 1286 s, 1269 s, 1193 s, 1176 s, 1096 w, 1051 m, 1027 m, 998 w, 916 s, 798 w, 775 w, 746 m, 718 w, 696 sh, 688 w, 582 w, 439 br.

[Ni$_8$(^{18}O$_2$)(abmo)$_6$(PhCO$_2$)$_2$(MeO)$_6$(MeOH)$_4$]·2MeOH (2A·2MeOH) from aboH$_2$ and ^{18}O$_2$. Manipulations were performed under argon in deoxygenated solvents using standard Schlenk techniques. To a slurry of Ni(PhCO$_2$)$_2$·3H$_2$O (0.4 mmol) and aboH$_2$ (0.4 mmol) in deoxygenated MeOH (25mL) was added a 1M Et$_3$N solution in EtOH (0.8 mmol). The slurry was stirred for 1 hour, during which time an orange-yellow precipitate formed in ~20% yield (based on Ni). The precipitate was filtered and the green filtrate was bubbled with a 250 mL of ^{18}O$_2$ (90%, ^{18}O-enriched). The solution turned dark-green brown and left undisturbed for 4 days. Dark green single crystals of **2A**·2MeOH were formed in ~63% yield (based on Ni). The crystals were collected by vacuum filtration, washed with a small amount of MeOH and Et$_2$O and dried in air. Analytical data, as well as IR data were identical to those of **2**·2MeOH.

[Ni$_8$(^{18}O$_2$)(abmo)$_6$(PhCO$_2$)$_2$(MeO)$_6$(MeOH)$_4$]·2MeOH (2A·2MeOH) from abmoH and H$_2$^{18}O$_2$. To a slurry of Ni(PhCO$_2$)$_2$·3H$_2$O (0.4 mmol) and abmoH (0.4 mmol) in MeOH (25mL) were added H$_2$^{18}O$_2$ (2-3% solution, 90% ^{18}O-enriched, 100 mg) and Et$_3$N (1M solution in EtOH, 0.8 mmol). The slurry was stirred for 1 hour. The resulting dark green-brown solution was left undisturbed for 4 days. Dark green single crystals of **2A**·2MeOH were formed in ~70% yield (based on Ni). The crystals were collected by vacuum filtration, washed with a small amount of MeOH and Et$_2$O and dried in air. Analytical data, as well as IR data were identical to those of **2**·2MeOH.

RESULTS AND DISCUSSION

Syntheses. The reaction of Ni(MeCO$_2$)$_2$·4H$_2$O with aboH$_2$ in MeOH and in the presence of triethylamine (Et$_3$N) at room temperature results in a yellow-orange powder and a dark green-brown solution. Recrystallization of the yellow-orange powder revealed the pentanuclear complex **4**, while slow evaporation of the dark green-brown solution afforded X-ray quality dark green crystals of **1**. Similar reactions involving Ni(PhCO$_2$)$_2$·3H$_2$O or Ni(4ClPhCO$_2$)$_2$ resulted in the same yellow-orange powder and X-ray quality dark green crystals of **2** and **3**, respectively. The identity of the products is independent of the metal to ligand ratio. Performing the same reactions at elevated temperatures (*i.e.* above 50 °C) substantially reduces the yield of complex **4** and increases the yields of complexes

1-3. With the structures of complexes **1-3** known, we repeated the same reactions in the absence of O_2: in this case only complex **4** forms and the solution does not turn dark green-brown, but retains its original green colour. In order to provide direct evidence that the μ_6-O_2^{2-} originates from the reduction of dioxygen we synthesized the ^{18}O-labelled complex **2** (**2A**) by the act of $^{18}O_2$ in a dioxygenated reaction mixture of **2**. The ^{18}O-labbeled **2A** was obtained and characterized by Raman spectroscopy. Non of the bands in the recorded spectra were sensitive to isotopic substitution of the peroxide, therefore we also performed ESI-MS on both unlabelled **2** and ^{18}O-labbeled **2A** where we observed a 4 units shift correlating to the labelling of both oxygens of the peroxo ligand. Having established the presence of the abmo$^-$ ligands within the cages of **1-3**, we attempted to isolate these complexes starting from abmoH instead of aboH$_2$. The solution does not turn dark green-brown until H_2O_2 is added to the reaction mixture in each case. As in the $Ni(RCO_2)_2$/aboH$_2$/Et$_3$N reaction system, the reactions of $Ni(RCO_2)_2$ with abmoH and H_2O_2 in MeOH in the presence of Et$_3$N results in dark green-brown solutions from which complexes **1-3** were isolated and their structures were re-confirmed by single-crystal X-ray crystallography. The ^{18}O-labbeled **2A** was also synthesized by adding $H_2^{18}O_2$ in a reaction mixture of $Ni(PhCO_2)_2 \cdot 3H_2O$/abmoH/Et$_3$N.

Description of structures. Although complexes **1-3** are not isostructural, their molecular structures are very similar. A labeled plot of representative complex **1**, whose structure will be discussed in detail, is shown in Figure 1 (see Supporting Information for figures of complexes **2** and **3**).

Complex **1** crystallizes in the triclinic space group P-1. The [Ni$_8$] cage is situated on a center of inversion and consists of a Ni$_6$(O$_2$) core with staggered symmetry (D_{3d}). The six Ni^{II} ions are situated at the apices of a distorted octahedron, with the Ni···Ni separations ranging from 3.362 to 4.856 Å. The octahedron is doubly face-capped by the remaining two Ni^{II} ions (Ni4 and Ni4'). All Ni^{II} ions are in distorted octahedral geometries. Six abmo$^-$ ligands bridge the central Ni$_6$ core in a η^1:η^1:η^1:μ-fashion, with each abmo$^-$ ligand chelating to one Ni^{II} ion through the carbonyl O atom and the oximato N atom and bridging to another through the deprotonated oximato O atom. Six μ_3-MeO$^-$ ligands (O71, O72 and O73) bridge the peripheral, face-capping Ni^{II} ions to the central core. The octahedral environment around these peripheral Ni^{II} ions is completed by two MeOH molecules and a terminal MeCO$_2^-$ ligand. Alternatively, the metal core of the octanuclear cage may be described as being composed of two "corner" sharing cubanes, with the shared "corner" being the μ_6-O_2^{2-} moiety (Figure 1). The presence of abmo$^-$ corroborates the absence of the hydrogen atom at the carbonyl carbon atom and the short C···O distance (i.e. 1.243(7), 1.246(7) and 1.253(6) Å for each of the three abmo$^-$ ligands) and the presence of a C=O bond. The η^3:η^3:μ_6-O_2^{2-} is fully surrounded by (six) Ni^{II} ions at the very center of the cage, and clearly templates the for-

mation of the octanuclear cluster. It would appear highly unlikely that the octanuclear metal cage would form first, before O_2^{2-} encapsulaltion. The O–O bond length in the peroxide is 1.487(4) Å, [1.508 Å in **2** and 1.491 Å in **3**] and is well within the limits of other reported peroxide bond lengths.[1-9] The Ni–O$_{peroxide}$ bond lengths are 2.055(3) Å, 2.031(3) Å and 2.015(3) Å for Ni1–O81, Ni2–O81 and Ni3–O81, respectively with the Ni–O$_{peroxide}$–Ni angles being 114.61(13)°, 97.58(12)° and 113.09(13)° for the Ni1–O81–Ni2, Ni1–O81–Ni3 and Ni2–O81–Ni3 angles, respectively. The Ni–O81–O81' angles are 111.47(19)°, 108.76(18)° and 111.03(19)° for Ni1, Ni2 and Ni3, respectively.
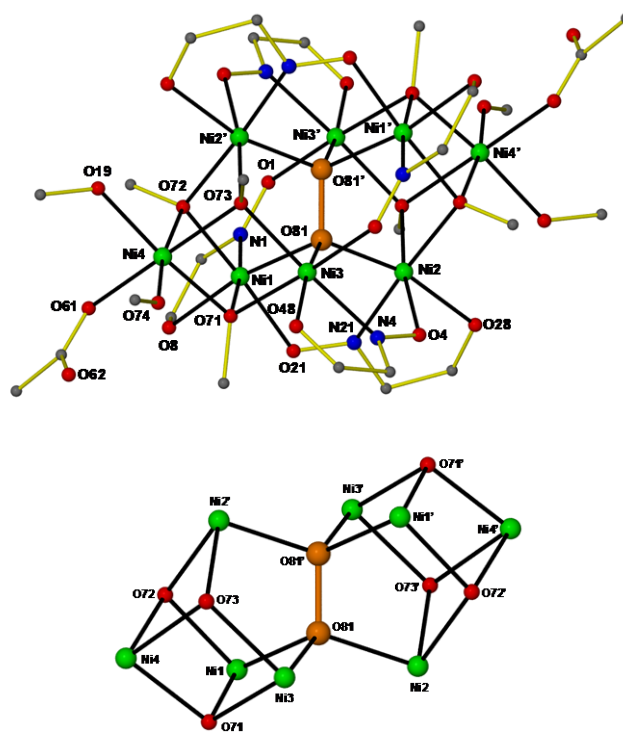

Figure 1. The structure of $[Ni_8(O_2)(abmo)_6(MeCO_2)_2(MeO)_6(MeOH)_4]$ **1** (top). All hydrogen atoms and most carbon atoms have been omitted for clarity. A view of the metal-oxygen core (bottom). Only the metal ions, the peroxide and the methoxide oxygen atoms are shown. Colour code: Ni green, C grey, N blue, O red. The η^3:η^3:μ_6-O_2^{2-} has been highlighted in orange. Symmetry code: (') -x, 1-y, -z.

Complexes **1-3** join a handful of structurally characterized abmoH complexes[12] and a very limited number of structurally characterized Ni^{II}-peroxo complexes.[5a,7a,7b,8] Indeed the related complex $[Ni_8(O_2)(L)_{12}](NO_3)_2$ (**5**; LH = N-substituted 3-hydroxy-2-pyridinone), is the only other reported example containing the η^3:η^3:μ_6-O_2^{2-} ion.[7a] The formation of this latter cluster was achieved only when H_2O_2 was added into the reaction mixture. The central Ni$_6$(O$_2$) core in **5** is similar to that seen for **1-3**, but with the two capping Ni^{II} ions residing in the faces of the octahedron lying in the same plane as the O_2^{2-} ion, rather than in the perpendicular plane for **1-3**. Other dissimilarities are the square pyramidal coordination geometry

around the central Ni[II] atoms and the absence of the MeO⁻ bridges.

Complex **4** (Figure 2) crystallizes in the triclinic space group *P*-1. The [Ni₅] cluster is situated on an inversion center and consists of five coplanar Ni[II] atoms, two abo²⁻ and six aboH⁻ ligands. The central Ni[II] atom (Ni1) is in a square planar geometry being chelated by the hydroxyl oxygen atoms and oximato nitrogen atoms from two $\eta^2{:}\eta^1{:}\eta^1{:}\mu_3$ abo⁻ ligands in a *trans* conformation. The hydroxyl O atom and the oximato O atom from both sides of the central Ni1 bridge Ni2 and its symmetry equivalent ion. Ni2 is in a distorted octahedral environment, being surrounded by a chelating aboH⁻ ligand and the hydroxyl oxygen atoms from a *cis*-[Ni(aboH)₂] subunit. The latter consists of a square planar Ni[II] ion (Ni3) being chelated by two $\eta^1{:}\eta^2{:}\mu$ aboH⁻ ligands through the hydroxyl oxygen atoms and the oximic nitrogen atoms in a *cis* configuration. Complex **4** is one of just a few structurally characterized aboH₂ complexes.[13]
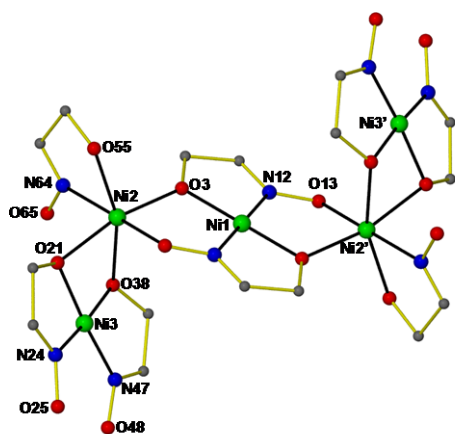

Figure 2. The structure of [Ni₅(abo)₂(aboH)₆] **4**. All hydrogen atoms and most carbon atoms have been omitted for clarity. Color code: Ni green, C grey, N blue, O red. Symmetry code: (') 1-x, -y, 1-z.

Raman Spectroscopy. The Raman spectra for the comparison of the ¹⁶O (**2**·2MeOH) and ¹⁸O (**2A**·2MeOH) complexes were collected for all samples on two different Raman spectrometers, both with 785 nm excitation. Although we used two different Raman spectrometers and varied both the exposure times and accumulation numbers in order to try and attain the optimal signal to noise (S/N) ratio in the Raman spectra we did not observe any shifts in the respective spectra in order to determine the peroxide stretching frequency (Figures S3 and S4 in the Supporting Information). Moreover, no Raman band was found to be sensitive to isotopic substitution with ¹⁸O in the known [Ni₈(O₂)(L)₁₂](NO₃)₂ cluster.[7a]

Mass spectrometry. Both the unlabelled (**2**) and ¹⁸O-labelled (**2A**) complexes were observed as both 1+ and 2+ species where one or both benzoate ligands were lost. A shift of 4 units was observed in the spectrum of **2A** compared to the spectrum of **2**, with this shift correlating to the labelling of both oxygens of the peroxo ligand (see

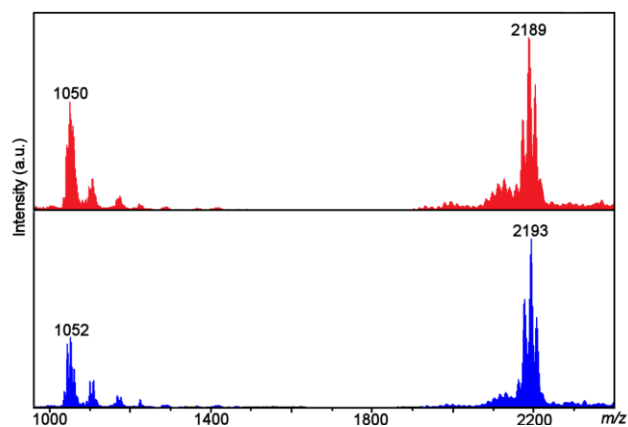Figure 3 and Tables 2 and 3 for mass spectra and assignments).

Figure 3. ESI-MS of **2** (top, red) and **2A** (bottom, blue) showing the observation of the unlabelled and ¹⁸O labelled [Ni₈] complex.

Magnetic Properties. Variable-temperature magnetic susceptibility data for the representative cage **1** were recorded between 250 and 5 K in an applied field of 1.0 kG. The plots of $\chi_M T$ versus T and χ_M versus T for **1** are shown in Figure 4. The $\chi_M T$ product for complex **1** decreases upon cooling from a value of 7.88 cm³ K mol⁻¹ at 250 K to a value of 0.76 cm³ K mol⁻¹ at 5 K. The shape of the curve as well as the low value of the $\chi_M T$ product at 5 K suggest the presence of dominant antiferromagnetic exchange interactions and a diamagnetic spin ground state. The experimental data were satisfactorily fitted using a simple one exchange parameter (*J*) model by employing spin Hamiltonian (1). The best fit parameters were *J* = −5.45 cm⁻¹ and *g* = 2.20.
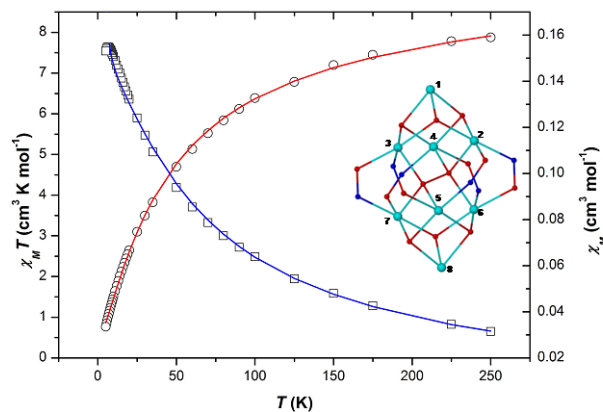

Figure 4. $\chi_M T$ vs. T (○) and $\chi_M T$ vs. T (□) plots for complex **1**. The solid red and blue lines represent fits of the experimental data to spin-Hamiltonian (1) and the the model shown in the inset - see text for details.

$$\hat{H} = -2J(\hat{S}_1{\cdot}\hat{S}_2 + \hat{S}_1{\cdot}\hat{S}_3 + \hat{S}_1{\cdot}\hat{S}_4 + \hat{S}_2{\cdot}\hat{S}_3 + \hat{S}_2{\cdot}\hat{S}_4 + \hat{S}_2{\cdot}\hat{S}_5 + \hat{S}_2{\cdot}\hat{S}_6 +$$
$$\hat{S}_3{\cdot}\hat{S}_4 + \hat{S}_3{\cdot}\hat{S}_5 + \hat{S}_3{\cdot}\hat{S}_7 + \hat{S}_4{\cdot}\hat{S}_5 + \hat{S}_4{\cdot}\hat{S}_6 + \hat{S}_4{\cdot}\hat{S}_7 + \hat{S}_5{\cdot}\hat{S}_6 + \hat{S}_5{\cdot}\hat{S}_7$$
$$+\hat{S}_5{\cdot}\hat{S}_8 + \hat{S}_6{\cdot}\hat{S}_7 + \hat{S}_6{\cdot}\hat{S}_8 + \hat{S}_7{\cdot}\hat{S}_8) \tag{1}$$

Thermal Properties. Complexes **1-3** are stable in the solid-state, can be handled in air and stored at room temperature as powdered samples or as single-crystals within

their mother liquor for a period of over two years. Thermogravimetric analysis (TGA, Figure 5) reveals that the three [Ni$_8$] cages are stable up to 200 °C. This is an abnormal behaviour for peroxide complexes[7a] and is attributed to the isolation of the μ_6-O$_2^{2-}$ within the cores of the [Ni$_8$] cages.
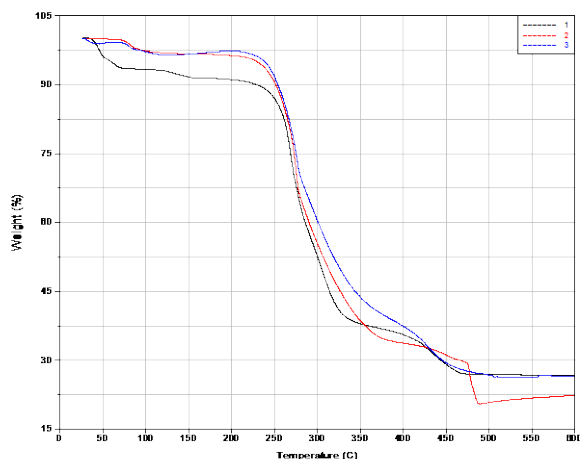

Figure 5. TGA plots in the 25 – 600 °C of **1-3**.

CONCLUSIONS

In summary, we report the synthesis and X-ray characterization of a family of octanuclear Ni^{II} cages which are templated by a rare η^3:η^3:μ_6-O$_2^{2-}$ produced by dioxygen activation. This is the first time the O$_2^{2-}$ (*i.e.* the reduced species) and the reducing agent for the O$_2$ reduction - which is not the metal ion - (*i.e.* the organic ligand found within the nickel cages in its oxidized form) were isolated and characterized by X-ray crystallography within the same compound(s). Cages **1-3** also represent unique paradigms of O$_2$ activation and reduction by Ni^{II} reaction blends, which means that the electrons needed to reduce the dioxygen into the O$_2^{2-}$ are not provided by the metal ion but by the organic ligand[2s,2t,2x] (*i.e.* aboH$_2$) which was found in its oxidized form (*i.e.* abmoH) within the cages. An alternative route providing access to the same [Ni$_8$] cages involves the use of the oxidized form of the ligand (*i.e.* abmoH) along with H$_2$O$_2$. The octanuclear cages are the first examples of polynuclear metal complexes which can be made from different organic ligands (*i.e.* aboH$_2$ and abmoH), and are exceptionally thermally stable (up to 200 °C). They also increase the number of the structurally characterized Ni^{II}-peroxo compounds from four[5a,7a,7b,8] to seven. The vibrational modes of the μ_6-O$_2^{2-}$ were not identified by Raman spectroscopy since no band was sensitive to isotopic substitution with ^{18}O; similarly no Raman band was found to be sensitive to isotopic substitution with ^{18}O in the known [Ni$_8$(μ_6-O$_2$)(L)$_{12}$](NO$_3$)$_2$ cluster.[7a] On the contrary, a shift of 4 units was observed in the ESI-MS spectrum of the ^{18}O-labelled **2A** compared to the spectrum of unlabelled **2**. This shift correlates to the labelling of both oxygens of the peroxo ligand, thus providing direct evidence that the peroxide originates from the reduction dioxygen. Magnetic susceptibility revealed relatively weak antiferromagnetic exchange inter-

actions between neighboring Ni^{II} ions, resulting in a diamagnetic spin ground state. The side product, a [Ni$_5$] cluster, was also isolated and characterized by X-ray crystallography. We are currently exploring the coordination chemistry of aboH$_2$ and abmoH with other 3d and 4f ions while examining the chemical reactivity of the [Ni$_8$] cages.

ASSOCIATED CONTENT

AUTHOR INFORMATION

Corresponding Author

ebrechin@staffmail.ed.ac.uk; gspapaef@chem.uoa.gr

ACKNOWLEDGMENT

REFERENCES

(1) (a) For a special issue on dioxygen activation by metalloenzymes and models, read: Nam W. (ed.) *Acc. Chem. Res.*, **2007**, *40*, 465-634. (b) For a forum on dioxygen activation and reduction, read: *Inorg. Chem.*, **2010**, *49*, 3555-3675.

(2) (a) Valentine, J. S. *Chem. Rev.* **1973**, *73*, 235-245. (b) Vaska L. *Acc. Chem. Res.* **1976**, *9*, 175-183. (c) Reim J.; Werner R.; Haase W.; Krebs B. *Chem. Eur. J.* **1998**, *4*, 289-298. (d) Cramer C. J.; Tolman, W. B.; Theopold, K. H.; Rheingold, A. L. *Proc.Nat. Acad. Sci.* **2003**, *100*, 3635-3640. (e) Kieber-Emmons, M. T.; Schenker, R.; Yap, G. P.; Brunold, T. C.; Riordan, C. G. *Angew. Chem. Int. Ed.* **2004**, *43*, 6716-6718. (f) Hikichi, S.; Okuda, H.; Ohzu, Y.; Akita, M. *Angew. Chem. Int. Ed.* **2009**, *48*, 188-191. (g) Liu, J. G.; Ohta, T.; Yamaguchi, S.; Ogura, T.; Sakamoto, S.; Maeda, Y.; Naruta, Y. *Angew. Chem. Int. Ed.* **2009**, *48*, 9262-9267. (h) Holland, P. L. *Dalton Trans.* **2010**, *39*, 5415-5425. (i) Sarangi, R.; Cho, J.; Nam, W.; Solomon, E. I. *Inorg. Chem.* **2011**, *50*, 614-620. (j) Yao, S.; Herwig, Y.; Xiong, C.; Company, A.; Bill, E.; Limberg, C.; Driess, M. *Angew. Chem. Int. Ed.* **2010**, *49*, 7054-7058. (k) Bochevarov, A. D.; Li, J.; Song, W. J.; Friesner, R. A.; Lippard, S. J. *J. Am. Chem. Soc.* **2011**, *133*, 7384-7397. (l) Cho, J.; Jeon, S.; Wilson, S. A.; Liu, L. V.; Kang, E. A.; Braymer, J. J.; Lim, M. H.; Hedman, B.; Hodgson, K. O.; Valentine, J. S.; Solomon, E. I.; Nam, W. *Nature* **2011**, *478*, 502-505. (m) Park, Y. J.; Ziller, J. W.; Borovik, A. S. *J. Am. Chem. Soc.* **2011**, *133*, 9258-9261. (n) Solomon, E. I.; Ginsbach, J. W.; Heppner, D. E.; Kieber-Emmons, M. T.; Kjaergaard, C. H.; Smeets, P. J.; Tian, L.; Woertink, J. S. *Faraday Discuss.* **2011**, *148*, 11. o) Tinberg, C. E.; Lippard, S. J. *Acc. Chem. Res.* **2011**, 44, 280-288. p) Boisvert, L.; Goldberg, K. I. *Acc. Chem.. Res.* **2012**, *45*, 899-910. (q) Maji, S.; Lee, J. C.; Lu, Y. J.; Chen, C. L.; Hung, M. C.; Chen, P. P.; Yu, S. S.; Chan, S. I. *Chem. Eur. J.* **2012**, *18*, 3955-3968. (r) Yao, S.; Driess, M. *Acc. Chem. Res.* **2012**, *45*, 276-287. (s) Dong, G.; Shaik, S.; Lai, W. *Chem. Sci.* **2013**, *4*, 3624-3635. (t) Dong, G.; Lai, W. *J. Phys. Chem. B* **2014**, *118*, 1791-1798.

(x) Fielding, A. J.; Lipscomb, J. D; Que L. *J. Biol. Inorg. Chem.* **2014**, in press: DOI: 10.1007/s00775-014-1122-9.

(3) (a) Latifi, R.; Tahsini, L.; Kumar, D.; Sastry, G. N.; Nam, W.; de Visser, S. P. *Chem. Commun.* **2011**, *47*, 10674-10676. (b) Zhou, M.; Crabtree, R. H. *Chem. Soc. Rev.* **2011**, *40*, 1875-1884. (c) Xiong, Y.; Yao, S.; Muller, R.; Kaupp, M.; Driess, M. *Nat. Chem.* **2010**, *2*, 577-580. (d) Citek, C.; Lyons, C. T.; Wasinger, E. C.; Stack, T. D. *Nat. Chem.* **2012**, *4*, 317-322. (e) Mirica, L. M.; Vance, M.; Rudd, D. J.; Hedman, B.; Hodgson, K. O.; Solomon, E. I.; Stack, T. D. *Science* **2005**, *308*, 1890-1892. (f) Reedijk, J. *Science* **2005**, *308*, 1876-1877. (g) Rolff, M.; Hamann, J. N.; Tuczek, F. *Angew. Chem. Int. Ed.* **2011**, *50*, 6924-6927.

(4) (a) Jeske, P.; Haselhorst, G.; Weyhermueller, T.; Wieghardt, K.; Nuber, B. *Inorg. Chem.* **1994**, *33*, 2462-2471. (b) Cozzolino, A. F.; Tofan, D.; Cummins, C. C.; Temprado, M.; Palluccio, T. D.; Rybak-Akimova, E. V.; Majumdar, S.; Cai, X.; Captain, B.; Hoff, C. D. *J. Am. Chem. Soc.* **2012**, *134*, 18249-18252. (c) Yokoyama, A.; Eun Han, J.; Cho, J.; Kubo, M.; Ogura, T.; Siegler, M. A.; Karlin, K. D.; Nam, W. *J. Am. Chem. Soc.* **2012**, *134*, 15269-15272. (d) Coggins, M. K.; Sun, X.; Kwak, Y.; Solomon, E. I.; Rybak-Akimova, E.; Kovacs, J. A. *J. Am. Chem. Soc.* **2013**, *135*, 5631-5640. (e) Lee, C. -M.; Chuo, Chen, C. -H.; Hu, C. -C.; Chiang, M. -H.; Tseng, Y. -J.; Hu, C. -H.; Lee, G. -H. *Angew. Chem. Int. Ed.* **2012**, *51*, 5427-5430. (f) Kim, K.; Lippard, S. J. *J. Am. Chem. Soc.* **1996**, *118*, 4914-4915. (g) Bouwman, E.; Driessen, W. L. *J. Am. Chem. Soc.* **1988**, *110*, 4440-4441. (h) Schmidt, S.; Heinemann, F. W.; Grohmann, A. *Eur. J. Inorg. Chem.* **2000**, 1657-1667. (i) Gavrilova, A. L.; Jin Qin, C.; Sommer, R. D.; Rheingold, A. L.; Bosnich, B. *J. Am. Chem. Soc.* **2002**, *124*, 1714-1722. (j) Leznoff, D. B.; Katz, M. J.; Cheng, L. K. L.; Draper, N. D.; Batchelor, R. J. *J. Mol. Struct.* **2006**, *796*, 223-229. (k) Givaja, G.; Volpe, M.; Edwards, M. A. Blake, A. J.; Wilson, C.; Schröder, M.; Love, J. B. *Angew. Chem. Int. Ed.* **2007**, *46*, 584-586. (l) Kodera, M.; Katayama, K.; Tachi, Y.; Kano, K.; Hirota, S.; Fujinami, S.; Suzuki, M. *J. Am. Chem. Soc.* **1999**, *121*, 11006-11007. (m) Meyer, F.; Pritzkow, H. *Angew. Chem. Int. Ed.* **2000**, *39*, 2112-2115.

(5) (a) Matsumoto, M.; Nakatsu, K. *Acta Cryst.* **1975**, *B31*, 2711-2713. (b) Yao, S.; Bill, E.; Milsmann, C.; Wieghardt, K.; Driess, M. *Angew. Chem. Int. Ed.* **2008**, *47*, 7110-7113.

(6) (a) Wilke, G.; Schott, H.; Heimbach, P. *Angew. Chem. Int. Ed.* **1967**, *6*, 92-93. (b) Otsuka, S.; Nakamura, A.; Tatsuno, Y. *J. Am. Chem. Soc.* **1969**, *91*, 6994-6999. (c) Fujita, K.; Schenker, R.; Gu, W.; Brunold, T. C.; Cramer, S. P.; Riordan, C. G. *Inorg. Chem.* **2004**, *43*, 3324-3326. (d) Kieber-Emmons, M. T.; Annaraj, J.; Sook Seo, M.; Van Heuvelen, K. M.; Tosha, T.; Kitagawa, T.; Brunold, C.; Nam, W.; Riordan, C. G. *J. Am. Chem. Soc.* **2006**, *128*, 14230-14231. (e) Kieber-Emmons, M. T.; Riordan, C. G. *Acc. Chem. Res.* **2007**, *40*, 618-625. (f) Company, A.; Yao, S.; Ray, K.; Driess, M. *Chem. Eur. J.* **2010**, *16*, 9669-9675.

(7) (a) Brown, E. J.; Duhme-Klair, A. K.; Elliott, M. I.; Thomas-Oates, J. E.; Timmins, P. L.; Walton, P. H. *Angew. Chem. Int. Ed.* **2005**, *44*, 1392-1395. (b) Cho, J.; Sarangi, R.; Annaraj, J.; Kim, S. Y.; Kubo, M.; Ogura, T.; Solomon, E. I.; W. Nam, *Nat. Chem.*, **2009**, *1*, 568-572. (c) Shiren, K.; Ogo, S.; Fujinami, S.; Hayashi, H.; Suzuki, M.; Uehara, A.; Watanabe, Y.; Moro-oka, Y. *J. Am. Chem. Soc.* **2000**, *122*, 254-262. (d) Cho, J.; Furutachi, H.; Fujinami, S.; Tosha, T.; Ohtsu, H.; Ikeda, O.; Suzuki, A.; Nomura, M.; Uruga, T.; Tanida, H.; Kawai, T.; Tanaka, K.; Kitagawa, T.; Suzuki, M. *Inorg. Chem.* **2000**, *46*, 2873-2885.

(8) Yao, S.; Xiong, Y.; Vogt, M.; Grutzmacher, H.; Herwig, C.; Limberg, C.; Driess, M. *Angew. Chem. Int. Ed.* **2009**, *48*, 8107-8110.

(9) (a) Auld, Jones, A. C.; Leese, A. B.; Cockayne, B.; Wright, P. J.; O'Brien, P.; Motevalli, M. *J. Mater. Chem.* **1993**, *3*, 1203-1208. (b) Hovnaninian, N.; Galloy, J.; Miele, P. *Polyhedron* **1995**, *14*, 297-300. (c) Sofetis, A.; Fotopoulou, F.; Raptopoulou, C. P.; Th. Zafiropoulos, F.; Perlepes, S. P.; Klouras, N. *Polyhedron* **2009**, *28*,

3356-3360. (d) Tolis, E. I.; Helliwell, M.; Langley, S.; Raftery, J.; Winpenny, R. E. P. *Angew. Chem. Int. Ed.* **2003**, *42*, 3804-3808.

(10) Catterick, J.; Thornton, P. *J. Chem. Soc. Dalton Trans.*, **1975**, 233-238.

(11) Taylor, T. W. J.; Marks, M. S. *J. Chem. Soc.* **1930**, 2302-2307.

(13) (a) Sharutin, V. V.; Molokova, O. V.; Sharutina, O. K.; Akimova, T. I.; Gerasimenko, A. V.; Pushilin, M. A. *Russ. J. Coord. Chem.* **2004**, *30*, 559-565. (b) E. Soleimani, *Rev. Chim.* **2009**, *60*, 484-487.

(14) (a) Karotsis, G.; Stoumpos, C.; Collins, A.; White, F.; Parsons, S.; Slawin, A. M.; Papaefstathiou, G. S.; Brechin, E. K. *Dalton Trans.* **2009**, 3388-3390. (b) Koumousi, E. S.; Manos, M. J.; Lampropoulos, C.; Tasiopoulos, A. J.; Wernsdorfer, W.; Christou, G.; Stamatatos, T. C.; *Inorg. Chem.* **2010**, *49*, 3077-3079. (c) Liu, S.; Zhu, H.; Zubieta, J. *Polyhedron* **1989**, *8*, 2473-2480. (d) Stamatatos, T. C.; Vlahopoulou, G.; Raptopoulou, C. P.; Psycharis, V.; Escuer, A.; Christou, G.; Perlepes, S. P. *Eur. J. Inorg. Chem.* **2012**, 3121-3131. (e) Vlahopoulou, G.; Stamatatos, T. C.; Psycharis, V.; Perlepes, S. P.; Christou, G. *Dalton Trans.* **2009**, 3646-3649.

Table 1. Crystallographic data for complexes 1-4

Compound reference	1·4H$_2$O	2·2MeOH	3	4·4MeOH·CH$_2$Cl$_2$
Chemical formula	C$_{98}$H$_{108}$N$_6$Ni$_8$O$_{32}$	C$_{110}$H$_{112}$N$_6$Ni$_8$O$_{30}$	C$_{106}$H$_{98}$Cl$_2$N$_6$Ni$_8$O$_{28}$	C$_{117}$H$_{112}$Cl$_2$N$_8$Ni$_5$O$_{20}$
Formula Mass	2351.58	2467.74	2444.48	2314.67
Crystal system	Triclinic	Monoclinic	Triclinic	Triclinic
a/Å	13.291(2)	13.259(2)	13.372(10)	12.8976(6)
b/Å	13.838(2)	28.761(5)	14.701(11)	13.0924(6)
c/Å	16.545(4)	15.273(3)	15.110(11)	16.4651(6)
α/°	108.734(3)	90.00	94.446(6)	98.686(3)
β/°	105.788(3)	103.829(2)	108.768(13)	99.661(3)
γ/°	101.737(2)	90.00	104.964(10)	90.904(3)
Unit cell volume/Å^3	2628.1(8)	5655.0(16)	2675(3)	2707.0(2)
Temperature/K	293(2)	296(2)	93(2)	150.0
Space group	$P\bar{1}$	$P2(1)/c$	$P\bar{1}$	$P\bar{1}$
No. of formula units per unit cell, Z	1	2	1	1
Radiation type	MoKα	MoKα	MoKα	Cu Kα
No. of reflections measured	17894	21909	26876	54794
No. of independent reflections	11581	8862	9695	9656
R_{int}	0.0352	0.0920	0.0381	0.0484
Final R_1 values ($I > 2\sigma(I)$)	0.0542	0.0631	0.0601	0.0686
Final $wR(F^2)$ values ($I > 2\sigma(I)$)	0.1391	0.1463	0.1644	0.1827
Final R_1 values (all data)	0.0933	0.1197	0.0623	0.0829
Final $wR(F^2)$ values (all data)	0.1603	0.1743	0.1669	0.2087
Goodness of fit on F^2	1.015	0.996	1.075	0.9640

Table 2. Assigned formulae for the unlabelled complex 2

m/z	Formula
1034	[Ni$_8$(O$_2$)(abmo)$_6$(MeO)$_6$(H$_2$O)$_2$]$^{2+}$
1041	[Ni$_8$(O$_2$)(abmo)$_6$(MeO)$_6$(H$_2$O)(MeOH)]$^{2+}$
1050	[Ni$_8$(O$_2$) (abmo)$_6$(MeO)$_6$(H$_2$O)$_2$(MeOH)]$^{2+}$
1059	[Ni$_8$(O$_2$) (abmo)$_6$(MeO)$_6$(H$_2$O)$_3$(MeOH)]$^{2+}$
2171	[Ni$_8$(O$_2$) (abmo)$_6$(PhCO$_2$)(MeO)$_6$(H$_2$O)]$^+$
2189	[Ni$_8$(O$_2$) (abmo)$_6$(PhCO$_2$)(MeO)$_6$(H$_2$O)$_2$]$^+$
2203	[Ni$_8$(O$_2$) (abmo)$_6$(PhCO$_2$)(MeO)$_6$(H$_2$O)(MeOH)]$^+$

Table 3. Assigned formulae for the ^{18}O-labelled complex 2A

m/z	Formula
1043	[Ni$_8$(^{18}O$_2$)(abmo)$_6$(MeO)$_6$(H$_2$O)(MeOH)]$^{2+}$
1052	[Ni$_8$(^{18}O$_2$) (abmo)$_6$(MeO)$_6$(H$_2$O)$_2$(MeOH)]$^{2+}$
1061	[Ni$_8$(^{18}O$_2$) (abmo)$_6$(MeO)$_6$(H$_2$O)$_3$(MeOH)]$^{2+}$
2175	[Ni$_8$(^{18}O$_2$) (abmo)$_6$(PhCO$_2$)(MeO)$_6$(H$_2$O)]$^+$
2193	[Ni$_8$(^{18}O$_2$) (abmo)$_6$(PhCO$_2$)(MeO)$_6$(H$_2$O)$_2$]$^+$
2207	[Ni$_8$(^{18}O$_2$) (abmo)$_6$(PhCO$_2$)(MeO)$_6$(H$_2$O)(MeOH)]$^+$

Table of Contents

aboH$_2$

abmoH

Ni(RCO$_2$)$_2$ / aboH$_2$ / Et$_3$N / O$_2$ $\longrightarrow$ **[Ni$_8$(O$_2$)(ambo)$_6$(RCO$_2$)$_2$(MeO)$_6$(solvent)$_4$]** $\longleftarrow$ Ni(RCO$_2$)$_2$ / abmoH / Et$_3$N / H$_2$O$_2$

[Ni$_5$(abo)$_2$(aboH)$_6$]